CapLibrate: Self-Calibration of an Energy Harvesting Power Supply with Supercapacitors

Christian Renner and Volker Turau
Institute of Telematics
Hamburg University of Technology
Hamburg, Germany
{christian.renner, turau}@tu-harburg.de

***Abstract*—Achieving perpetual and self-sustaining operation of wireless sensor nodes is an important topic of current research in the field of energy harvesting. Closely related to this is the employment of energy budgeting, i.e., effective utilization of available and future energy resources without pushing a node towards the hazard of energy depletion. Therefore, reliable prediction of node lifetime in context of the available energy within a given time is required. This in turn requires self-calibration of the sensor nodes and their energy harvesting supply. In this paper, we explore and assess models for a supercapacitor-based harvesting supply. The parameters of the models are discussed and determined, so that fast, reliable, and energy-efficient calibration becomes possible. Moreover, measurement results for a specific hardware platform are discussed and a roadmap for a self-calibration algorithm is presented.**

I. Introduction

Perpetual operation of wireless devices, such as wireless sensor nodes, is a research goal being addressed with increasing frequency. First steps on this ground were focusing on energy-efficiency. Despite the importance of this approach, it can merely prolong a sensor node's lifetime, yet energy depletion will eventually occur. For battery capacities are not expected to rise in orders of magnitude within the near future, provided that larger-sized batteries are not an option, and since replacement of batteries is usually infeasible, research ought to embark on a different strategy.

Recent works have investigated the potential of harvesting energy from the environment and pointed out its feasibility. Various harvesting solutions can be employed, among the sources being sunlight, radio frequency, wind, vibration, or temperature differences. Particularly sunlight is highly promising, since it produces a sufficient amount of energy to supply wireless sensor nodes, which draw currents between several μA in the sleep state and some mA in full-operation mode.

Unfortunately, the amount of harvested energy is scarcely constant or continuous. In case of solar harvesting, energy can exclusively be gathered during daytime and additionally depends on weather conditions and the time of the year. As a result, energy must be buffered, so that nodes do neither suffer from temporal energy shortage nor is their operation restricted to periods of incoming energy.

Various energy buffers are available on the market and many more are yet to come, but most solutions exhibit a considerable drawback: the stored energy reserve cannot be estimated in an easy and precise manner. However, this ability is required in order to allow for what we refer to as *energy budgeting*. The latter handles the problem of performing application tasks in a way that a given amount of energy per time—the energy budget—is used effectively. This implies that as many tasks as possible are scheduled, such that the needs and return of the application are maximized while the energy budget is not exceeded. Techniques with this respect embrace adaptive duty-cycling and energy-aware scheduling, i.e., shrinking the probability of accidental energy depletion caused by running a highly energy-consuming task during periods of low energy reserves.

For energy budgeting it is crucial that the size of the energy budget can be determined precisely at any time. This implies an exact knowledge of various system parameters. Firstly, the capacity of the energy buffer must be determined with an accuracy of a few percent, since any error of its value leads to an error of the same magnitude for budget estimation. In order to schedule tasks, the power profile of the sensor node and the efficiency of the circuit must be identified, since they have the same impact as the capacity value. A strict claim for these two determinations is that they have to be performed with little energy cost and without interrupting normal operation of the node.

Within the last couple of years, a new and promising energy storage technology has become available: electric double-layer capacitors—also called supercapacitors—with high capacities. They fill the gap between capacitors and rechargeable batteries and can store enough energy to keep modern sensor nodes alive for a couple of days without recharging. Their main advantage over rechargeable batteries is the high number of possible charge-discharge cycles. While a lifetime of 2-3 years can be expected for lithium-ion polymers, supercapacitors can last for 10 years or even more. Supercapacitors do not need a complex charging circuit and render easy estimation of their energy reserves possible. We have gained experience with supercapacitors in a self-developed solar energy-harvesting power-supply [1], that is equipped with Panasonic Gold-Caps [2] and SAMWHA GreenCaps [3]. The main outcome of our effort are models for lifetime prediction of sensor nodes based on the available energy resources stored in the supercapacitor.

Unfortunately, the actual capacity of supercapacitors is

subject to manufacturing variations and also degenerates with supercapacitor age and environmental temperature changes. These may be as large as 30% [3] of the initial value. Since manual determination and state-tracking of the actual capacity is not feasible, an automated mechanism is mandatory. Devices must be able to perform self-calibration, encompassing initial determination and dynamic updating of the actual capacity, so that a reliable estimation of the available energy reserves is achieved and maintained. In this paper, we present our progress in this field. We develop and evaluate mathematical models and propose algorithms for autonomic capacity determination and adaptive updating in order to improve the preciseness of the already proposed lifetime prediction methods. We exploit these findings to additionally propose a procedure for self-calibration of wireless sensor nodes equipped with a supercapacitor-based energy harvesting supply.

First, we will discuss related work in Sect. II. In Sect. III the hardware platform is introduced and lifetime prediction techniques and requirements are revisited. Theoretical models of capacity estimation are presented in Sect. IV, enriched by considerations on practicability presented in Sect. V. Afterwards, these models are evaluated and discussed in Sect. VI, before the paper is concluded in Sect. VII.

II. Related Work

Various self-sustaining power supplies for wireless sensor nodes have been introduced in the past. The Enviromote [4] is a platform equipped with a solar cell as its power source and NiMH batteries for energy storage. Easy circuit design and cheap energy storage devices are its main design goals. The authors present charging and discharging characteristics of their power supply. A solar harvesting supply with lead acid batteries for the IRIS [5] platform is developed in [6]. The circuit is designed to operate the solar cell at a static maximum power point.

Another platform employing a solar cell is Prometheus [7]. It is based on a two-stage energy storage system consisting of a supercapacitor as the primary energy source and a rechargeable Li^+ battery. The supercapacitor conserves the battery by limiting its charging and discharging cycles. In the corresponding paper, charging and discharging behavior of the circuit and supercapacitors are examined. The authors take a first step into the direction of energy-aware scheduling by adapting the duty cycle to the current supercapacitor voltage. Prometheus has been successfully deployed in the Trio testbed [8].

The Everlast platform stores energy harvested by a solar cell in a supercapacitor solely [9]. Maximum power point tracking (MPPT) is employed in order to increase the efficiency of the solar cell, i.e., the electrical power produced by the cell is maximized. The authors claim that their platform can operate for up to 20 years while preserving high data rates.

These projects illustrate the relevance of supercapacitors in novel wireless sensor network platforms and applications. Despite this fact, dynamic lifetime prediction based on the stored energy and therefore energy budgeting has not been employed yet. A first approach towards an energy neutral operation of sensor networks is presented by Kansal et al. [10]. They have developed abstractions to characterize the complex time varying nature of self-sustaining energy sources with analytically tractable models including an energy prediction model. To the best of our knowledge the usage of energy budgets has not been considered in the literature. In fact none of the sensor networks discussed in the survey about solar powered sensor networks by Jeong et al. makes use of such a concept [11].

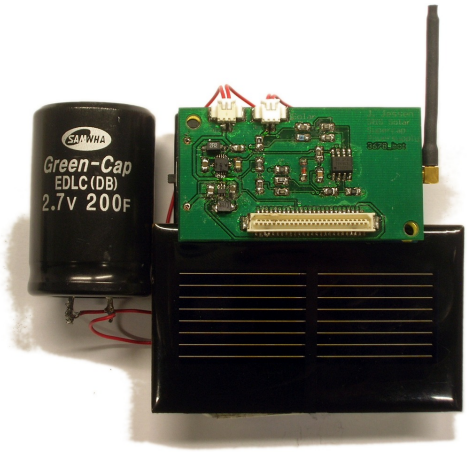

Fig. 1. Energy Harvesting Platform for the IRIS node

To set a fully operational energy-budgeting system with supercapacitors into practice, a more detailed understanding of the characteristics of supercapacitors is needed. Barrade and Rufer discuss the energy density and power density of supercapacitors [12]. For this purpose, they derive analytical models for the discharging behavior. Yet, estimation techniques for capacitance determination have not been discussed and evaluated for wireless sensor networks to the best of our knowledge, though it is fundamental for reliable energy budgeting.

III. Energy Harvesting System

In this section, the hardware platform under consideration is introduced and the main results of prior work, constituting the fundament of this contribution, are sketched.

A. Power-Supply Hardware

The energy harvesting platform is an evolution of the one presented in [1]. It supplies an IRIS sensor node from Crossbow Technology [5] with a supercapacitor as its energy buffer. While the harvesting module still uses a solar cell as its energy source, the input is decoupled from the energy buffer by a TPS61200 DC-DC buck-boost converter from Texas Instruments [13]. The converter keeps the solar cell in a static maximum power point and prevents the supercapacitor from discharging during times of insufficient sunlight. A complete setup with an IRIS node, the harvesting board, a supercapacitor, and a solar cell is depicted in Fig. 1

The discharging circuit consists of the Texas Instruments DC-DC buck-boost converter TPS61221 [14], which ensures

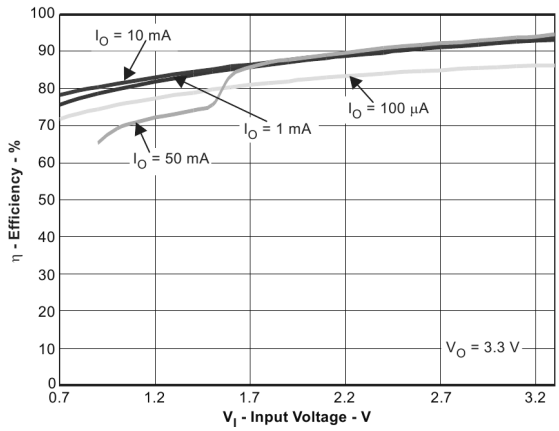

Fig. 2. Efficiency versus input voltage and output current of the TPS61221 [14]

a stable and constant supply voltage of $3.3\,\mathrm{V}$. The converter starts converting at an input voltage of $0.7\,\mathrm{V}$, has a low quiescent current of $5.5\,\mu\mathrm{A}$, and a high efficiency for the expected power profile. Figure 2 depicts the efficiency for different output currents and input voltages. As the input of the converter is directly connected to the supercapacitor, the input voltage ranges from $0.7\,\mathrm{V}$ to $2.7\,\mathrm{V}$. For node-operation in full-power mode with a current of a few mA the efficiency of the converter will be higher than 80%. Even in sleep mode with a current of a few $\mu\mathrm{A}$, the efficiency will remain well above 60%.

B. Lifetime Prediction

One of the major design criteria of the energy harvester presented above is its ability to easily and reliably estimate the energy reserve. For this reason, the supercapacitor technology was chosen as the energy buffer. As we have previously shown in [1], lifetime prediction is possible by application of the simplified equation

$$T_{\mathrm{life}} = \frac{\eta C}{2P_{\mathrm{N}}}\left(V_{\mathrm{C}}^2 - V_{\mathrm{min}}^2\right). \tag{1}$$

In this equation, T_{life} is the expected remaining lifetime of the sensor node for a power consumption of P_{N} with a constant conversion efficiency of η. The capacitance of the supercapacitor is C, while V_{C} and V_{min} denote the current capacitor voltage and converter cut-off voltage, respectively.

We have also introduced and evaluated a more accurate but also more complex prediction method. Since it takes into account the self-discharge of the supercapacitor, which can barely be neglected when the supercapacitor voltage V_{C} is close to its maximum, the quality of lifetime prediction is increased. However, the general gain of preciseness that can be drawn from this improved equation falls short to the impact of another source of impreciseness: the actual capacitance of the supercapacitor. As can be seen in (1), it influences lifetime prediction linearly. A look at the data sheets reveals that the actual capacitance can deviate from the rated value by as much as $\pm 30\%$ [3]. Capacitance decreases with the supercapacitor's age and the environment temperature. Therefore arises the need to reliably estimate and update the actual value of the capacitance. Since sensor networks are envisioned to consist of hundreds or thousands of nodes, this can not be done manually. Furthermore, the timely change of capacitance renders capacitance determination prior to node deployment useless on the long run. As a result, methods of capacitance determination and online estimation have to be devised, assessed, and cast in an autonomous piece of software. A fair amount of the way towards this goal is covered in this paper.

IV. Capacity Determination

To achieve the goal of autonomous self-calibration of the harvesting supply regarding the capacity of the energy buffer, we present and discuss different approaches in this section. All of these do not take self-discharge into consideration, for it has a noticeable impact on the behavior of the supercapacitors for voltages close to the maximum rating only (cf. [1]). Moreover, we assume that there is no incoming energy during self-calibration, i.e., the solar cell is detached or temporarily disconnected via an electric switch.

A. Resistance Discharging

Aiming at pure determination of the capacity C of a supercapacitor, the straight forward way is to connect a resistance R (see Fig. 3). Using this setup, the voltage drop ΔV_{C} during the period ΔT can be assessed by applying the following equation:

$$V_{\mathrm{C}} = V_{\mathrm{C0}} \cdot \mathrm{e}^{-\frac{\Delta T}{RC}}. \tag{2}$$

Here, V_{C0} denotes the reference voltage at time T_0 while $V_{\mathrm{C}} = V_{\mathrm{C0}} - \Delta V_{\mathrm{C}}$ is the voltage at time $T = T_0 + \Delta T$. Our findings from [1] indicate that assuming an ideal capacitance is valid for the scenario under investigation, so that a more complex equivalent circuit is not employed.

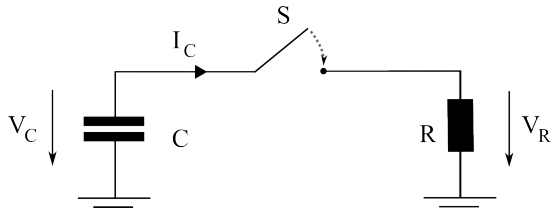

Fig. 3. Stand-alone discharging circuit with resistance R

The final equation to estimate the capacity is

$$C = \frac{\Delta T}{R} \cdot \ln^{-1}\left(\frac{V_{\mathrm{C0}}}{V_{\mathrm{C}}}\right). \tag{3}$$

B. Converter Discharging

Another way to determine the capacity of a supercapacitor is to consider the circuitry as presented in Sect. III-A. In this case a DC-DC converter with a known and fixed output power P_{N} is used as the load. As this same converter already powers the node itself, no extra hardware or circuitry is required. The schematic of this setup is shown in Fig. 4. This approach introduces another inaccuracy by means of the efficiency η

of the converter. Unfortunately, η is not constant for a given output power, as it also depends on the input voltage, i.e., the capacitor voltage V_C. The following considerations are therefore only valid for small changes of V_C, which allow for the assumption of a constant η.

The amount of energy stored in a capacitor is

$$E_\mathrm{C} = \frac{1}{2} C V_\mathrm{C}^2, \tag{4}$$

and the energy consumed by the converter in the period ΔT can be expressed as

$$E_\mathrm{out} = \Delta T \cdot \eta^{-1} \cdot P_\mathrm{N} \tag{5}$$

Within the same period ΔT, the energy expenditure E_out is also experienced by the supercapacitor and reflected by a voltage drop ΔV_C. Starting with an initial voltage $V_{\mathrm{C}0}$, a runtime of ΔT will lead to the new voltage $V_\mathrm{C} = V_{\mathrm{C}0} - \Delta V_\mathrm{C}$. Employing this knowledge in (4), combining with (5) and finally solving for C gives

$$C = \frac{2 \cdot \Delta T \cdot P_\mathrm{N}}{\eta \cdot \left(V_{\mathrm{C}0}^2 - V_\mathrm{C}^2\right)} \tag{6}$$

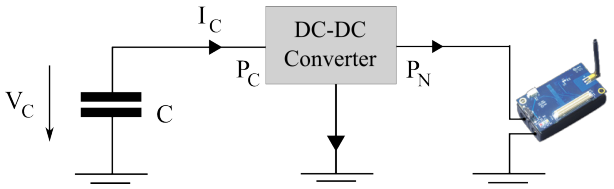

Fig. 4. Discharging circuit with a DC-DC converter and an IRIS node [5]

C. Combined Discharging

If resistance discharging (cf. Sect. IV-A) shall be performed by the sensor node itself, the two aforementioned models must be combined. To derive a mathematical model, V_C from (2) is used to calculate the amount of energy consumed by the resistor R:

$$E_R = \frac{V_{\mathrm{C}0}^2}{R} \int_0^{\Delta T} \mathrm{e}^{-\frac{2t}{RC}}\,\mathrm{d}t = \frac{C V_{\mathrm{C}0}^2}{2} \cdot \left(1 - \mathrm{e}^{-\frac{2\Delta T}{RC}}\right) \tag{7}$$

From $\Delta E_\mathrm{C} = E_\mathrm{out} + E_R$ and (4) plus (5) then follows

$$C \cdot \left(V_{\mathrm{C}0}^2 \cdot \mathrm{e}^{-\frac{2\Delta T}{RC}} - V_\mathrm{C}^2\right) = \frac{2 \cdot \Delta T \cdot P_\mathrm{N}}{\eta} \tag{8}$$

However, there is no simple analytical solution for this expression, because C is present as a factor and in the exponential term on the left-hand side of the equation. In particular, this implies that the equation cannot be solved by a sensor node's low computing-power microprocessor. Yet, if $\frac{P_\mathrm{N}}{\eta}$ is small compared to the power of the resistor, it can be neglected and (8) can be reduced to (3).

V. Application

To bring theory from the previous section into practice, deliberations about circuitry layout and part dimensions must be undertaken. Furthermore, reasonable and effective values for ΔT and ΔV_C must be determined, while the effect of measurement impreciseness and calculation errors have to be considered. These issues are addressed in this section.

There exist two important application scenarios for self-calibration: during a self-calibration phase at node boot time and after expiration of service intervals that are intended to cope with changes of the actual capacitance. In the first case, there are generally no time constraints, if the nodes are deployed sufficiently early enough, i.e., self-calibration is completed before the planned, normal application start. Contrarily, adaptation of the capacitance should be a fast process in order to not interfere with the node's normal application. We will therefore discuss the time needed to achieve calibration results that are as accurate as possible.

A. Discharging Parameters

For resistance discharging, the resistor has to be picked to allow for fast discharging in order not to disturb regular node operation. This implies a low resistance value. Another benefit of a small resistance and thus large current is that the sleep power of the node (and the DC-DC-converter) becomes negligible. However, we think it is also important choosing the resistance in an order of magnitude reflecting a node's actual current consumption. Doing so prevents measurements from being influenced by possible dependencies on the latter. Hence, we picked resistances of values $R = 10\,\Omega$ and $R = 40\,\Omega$, for which the current ranges from $270\,\mathrm{mA}$ down to $25\mathrm{mA}$ for $0.7\,\mathrm{V} \leq V_\mathrm{C} \leq 2.7\,\mathrm{V}$. Timing characteristics for these resistance values are compiled in Table I. If the current drawn from the capacitor should follow the node's current profile, $R = 40\,\Omega$ is preferable. Then it is evident from the values that only for $\Delta V_\mathrm{C} = 0.1\,\mathrm{V}$ a very short calibration phase is achieved for capacitances of up to $200\,\mathrm{F}$. To improve measurement precision, high precision resistors are required, as they influence overall precision linearly. To achieve better accuracy than the tolerances noted in the supercapacitor data sheets, we recommend tolerances of at most 1%.

In case of converter discharging, the actual efficiency of the whole circuit has to be known. Since the main point of power loss is expected to be the DC-DC-converter, the approximate efficiency values can be from its data sheet. Unfortunately, the data sheet does not give exact values for a current of ca. $15.8\,\mathrm{mA}$ that is drawn by the IRIS platform with a switched on but idle transceiver; but the provided plot for $10\,\mathrm{mA}$ serves as an orientation point. For $0.7\,\mathrm{V} \leq V_\mathrm{C} \leq 2.7\,\mathrm{V}$, the efficiency rises almost linearly from roughly 75% to 92%. The time needed to generate a voltage drop of $0.1\,\mathrm{V}$ is displayed in Table II. Apparently, discharging a $200\,\mathrm{F}$ supercapacitor is quite time consuming, whereas capacity determination of a small capacitor can be achieved quickly. Moreover, the voltage drops faster for small reference voltages $V_{\mathrm{C}0}$, so that capacity estimation can be carried out faster. This is caused

V_{C0}	ΔV_C	ΔT(min) for diff. $R \cdot C$ combinations			
		10 Ω, 25 F	40 Ω, 25 F	10 Ω, 200 F	40 Ω, 200 F
2.5 V	0.1 V	0:10	0:41	1:22	5:27
	0.3 V	0:32	2:08	4:16	17:03
	0.5 V	0:56	3:43	7:26	29:45
2.0 V	0.1 V	0:13	0:51	1:43	6:50
	0.3 V	0:41	2:43	5:25	21:40
	0.5 V	1:12	4:48	9:35	38:21
1.5 V	0.1 V	0:17	1:09	2:18	9:12
	0.3 V	0:56	3:43	7:26	29:45
	0.5 V	1:41	6:45	13:31	54:04

TABLE I
TIMING FOR RESISTANCE DISCHARGING FOR DIFFERENT ΔV_C

V_{C0}	η	ΔT(min) for diff. C	
		25 F	200 F
2.5 V	91%	1:47	14:16
2.0 V	88%	1:12	10:59
1.5 V	85%	0:59	7:53

TABLE II
TIMING OF CONVERTER DISCHARGING FOR $\Delta V_C = 0.1\,\mathrm{V}$ AND $P_N = 52.1\,\mathrm{mW}$

by two reasons. Firstly, the converter efficiency declines with decreasing input voltage. Secondly, the input voltage follows a square-root shape. This result has been derived and discussed in a previous paper [1].

The theoretical analysis of the discharging behaviors indicates that a voltage drop of $0.1\,\mathrm{V}$ should be considered the maximum in order to achieve fast estimations (less than $10\,\mathrm{min}$), so that the application of the node is not disturbed massively. Furthermore, resistance discharging is much faster for larger reference voltages V_{C0}, but slower for smaller ones. In conclusion, the resistance method shows to be more practical in the first case, but converter discharging is preferable in the second one. For resistance discharging, $R = 40\,\Omega$ is a good choice, allowing for both fast discharging (and thus capacity-estimation) times and adhering to the current consumption of many sensor nodes.

B. Measurement Precision

When calculating dimensions from measured values, the latter are prone to impreciseness caused by measurement error. This issue is discussed in the following.

The heart of the IRIS platform is the Atmel ATmega 1281 microcontroller with 10 bit ADC ports that are configured to use the node supply voltage V_N as reference. Therefore, measurement resolution is $r = V_N/1024$ with a quantization error of $\pm V_N/2048$. According to the data sheet absolute accuracy is $\pm 2\,LSB$, i.e., $\pm 3r$. As ADC readings are therefore generally afflicted with an error of absolute value ε, the computed quantities will not be correct either. In order to judge the preciseness and reliability of the obtained values, the maximum errors have to determined. Recall that the error of capacity estimation has linear influence on lifetime prediction.

For resistance discharging, the relative error becomes

$$\left|\frac{C-\widetilde{C}}{C}\right| \overset{(3)}{=} \left|1 - \frac{\ln\left(1-\Delta V_C/V_{C0}\right)}{\ln\left(1-\widetilde{\Delta V_C}/\widetilde{V_{C0}}\right)}\right| \leq \frac{\ln\left(\frac{V_{C0}}{V_{C0}-\Delta V_C}\cdot\frac{V_{C0}-\Delta V_C-3\varepsilon}{V_{C0}-\varepsilon}\right)}{\ln\left(\frac{V_{C0}-\Delta V_C+3\varepsilon}{V_{C0}+\varepsilon}\right)} \tag{9}$$

For $1\,\mathrm{V} \leq V_{C0} \leq 2.5\,\mathrm{V}$ and ΔV_C the relative error of C is at most 3.6% for $\varepsilon = V_N/2048$. By taking a few consecutive measurements and averaging them, this error can be reduced. For an error of $\varepsilon = 3r$ measurement preciseness melts further down, as the relative error increases to a theoretical maximum of 26.4%.

The relative error for converter discharging is

$$\left|\frac{C-\widetilde{C}}{C}\right| \overset{(6)}{=} \left|1 - \frac{V_{C0}^2 - V_C^2}{\widetilde{V_{C0}}^2 - \widetilde{V_C}^2}\right| \leq \frac{2\varepsilon\left(2V_{C0}-\Delta V_C\right)}{2V_{C0}\Delta V_C - \Delta V_C^2 - 2\varepsilon\left(2V_{C0}-\Delta V_C\right)}. \tag{10}$$

Here, the relative error is less than 3.4% for the same setup. Again, averaging is the method of choice to increase reliability. When considering the absolute accuracy of the ADC in use, the relative error increases to a theoretical maximum of 24.0%.

The relative error induced by quantization is acceptable, as it is way smaller than the possible deviation of the actual capacity. In contrast, the theoretical maximum with respect to the absolute accuracy of the ADC appears severe; yet, the values obtained stem from the hypothetical worst case scenario, which we expect to rarely happen in praxis. Furthermore, increasing ΔV_C is a poor option, since it prolongs measurement time severely, although doubling would cut the error down by more than half. We will therefore stick to the choice of $\Delta V_C = 0.1\,\mathrm{V}$ and leave it up to the evaluation of actually measured results, whether this choice is sound.

With these results in mind, the good news is that the IRIS platform uses an external oscillator to increase timing precision to some ten parts per million. Hence, timing errors can be neglected for large values of ΔT (in the order of a few minutes).

C. Calculation Errors

When performing the calculations required in (3) and (6), additional sources of errors are introduced. Firstly, the Atmel 1281 does not support floating point operations. These can be emulated by the software, but this infers computational overhead and an increased program size. As a result, 8-bit or 16-bit integers can be used to emulate fixed-point operations. Particularly divisions must then be handled carefully so as to preserve as much precision as possible. Secondly, mathematical functions—in particular, the logarithm present in (3)—are not available and have to be approximated. To keep computing overhead low, interpolation with look-up tables is a possible

approach; yet, the preciseness of the results must be smaller than the expected deviation of the actual capacity from the nominal value, i.e., within a few percent.

The previous remarks are for completeness only, because we will only perform offline computations in the remainder of this paper. Online estimation, i.e., self-calibration of sensor nodes, is current work in progress.

VI. Evaluation and Discussion

In this section, results from various test series according to the methods proposed and discussed in Sect. IV are presented and evaluated. Based on this, the different approaches of capacity determination are assessed. This knowledge is finally exploited to devise a roadmap for online capacitance determination.

A. Offline Capacitance Determination

Before devising algorithms for online capacitance estimation, the underlying methods as presented in Sect. IV have been evaluated. For this purpose, a simple measurement application has been written for the IRIS platform using TinyOS 2.1. The software starts a series of four ADC conversions of the supercapacitor voltage with a period of $1\,\mathrm{min}$. The average of each four readings is immediately sent via the radio to a base station, which simply forwards the data over the serial line to a computer, where the data is logged.

We have conducted three different measurement setups that will be explained in the following along with assessing the obtained results. In each of these setups, the IRIS node is supplied by the harvesting power-supply board described in Sect. III-A. The supply voltage of the node is $V_\mathrm{N} = 3.3\,\mathrm{V}$.

For all measurements, GreenCaps [3] with rated capacities of 25, 100, and $200\,\mathrm{F}$ were used and fully charged to their maximum voltage of $V_{\mathrm{C}0} = 2.7\,\mathrm{V}$. Capacity estimation is performed with reference voltages of $V_{\mathrm{C}0} = 1.5, 2.0, 2.5\,\mathrm{V}$.

Since voltages have been recorded in the same intervals for all capacitors, data points become closer the higher the capacity is. This explains the observable ripples in all capacity estimation plots for larger capacities plus late starting points for the smallest capacitor.

1) Stand-alone Resistance Setup: In this setup, the node is supplied separately, i.e., the power input of the harvester is connected to a battery pack. The supercapacitor is solely attached to one of the ADC inputs of the IRIS node and discharged with a resistance R. The intention of this setup is to measure unbiased values of the actual capacitance of the supercapacitors. It is a valid reference for analyzing the impact—or introduced error—by the other two methods, but no realistic deployment setup.

The results for $R = 36.1\,\Omega$ are depicted in Fig. 5, whereas the ones for $R = 10.1\,\Omega$ are omitted as they yield qualitatively the same results. As expected, voltage (Fig. 5a) decreases exponentially for the three capacitors, where the (nominal) capacity has linear influence on discharging time—e.g., the $1\,\mathrm{V}$mark is reached after approximately $15\,\mathrm{min}$, $60\,\mathrm{min}$, and $120\,\mathrm{min}$ for the different supercapacitors. Hence, assuming ideal capacitive behavior is valid.

The results of capacity estimation using (3) is shown in Fig. 5b. In general, the estimated values are close to the nominal ones. In more detail however, a few phenomena can be observed. Firstly, the capacity increases with rising ΔV_C, which is most likely due to the vanishing presence of leakage current for smaller values of V_C (cf. [1]). Therefore, estimated capacity values of smaller reference voltages $V_{\mathrm{C}0}$ are slightly larger. Although the differences are merely marginal, the results of $V_{\mathrm{C}0} = 1.5\,\mathrm{V}$ and $V_{\mathrm{C}0} = 2.0\,\mathrm{V}$ show a better match than those for $V_{\mathrm{C}0} = 2.0\,\mathrm{V}$ and $V_{\mathrm{C}0} = 2.5\,\mathrm{V}$. Secondly, a small voltage drop is sufficient to achieve estimations with accurate capacity estimations, i.e, estimations settle down within less than $\Delta V_\mathrm{C} = 0.1\,\mathrm{V}$ in most cases. The expectations from Sect. V-B are thus validated.

These findings allow for the conclusion that capacity estimation for supercapacitors with the resistance method is possible and also reliable. Due to the influence of leakage current, the capacity is slightly smaller for larger values of $V_{\mathrm{C}0}$ and small values of ΔV_C. However, this causes no real harm, since underestimation of the capacity will lead to an underestimated lifetime. In order to achieve more accurate results we suggest capacity estimation for values of $V_{\mathrm{C}0} \approx 2.0\,\mathrm{V}$. This magnitude also aims at preserving as much energy as possible after a completed estimation, so that node operation is not jeopardized in case of poor future harvesting capabilities.

2) Combined Resistance Setup: In contrast to the previous setup, the supercapacitor now supplies the sensor node, and it is still connected to one of the node's ADC inputs and discharged with a resistance $R = 35.6\,\Omega$. The node's radio is generally switched off and the node is in the sleeping mode. After each series of ADC conversions, the radio is briefly switched on in order to transmit the voltage sample to the base station, and it is switched off immediately afterwards.

The resistance can be switched via an IO-pin driving a Vishay Siliconix Si9410BDY MOSFET [15], which is wired as depicted in Fig. 6. The maximum drain current of the discharging circuit is large enough to conserve the expected exponential voltage decrease of the capacitor. In our measurement setup, the resistance is activated right after the completed booting process of the node.

Since the sensor node switches its radio on for only a few milliseconds every second, overall energy consumption of the node is low as compared to the power drawn be the resistance. Therefore, capacity estimation is performed using (3) instead of the more complex (8). The results are shown in Fig. 7.

The voltage in Fig. 7a behaves as already observed in Fig. 5a. In particular, the $1\,\mathrm{V}$ break-throughs are almost the same as for the plain resistance setup, so that using the simplified capacity estimation equation will not lead to significant estimation errors. For this reason, the estimation values displayed in Fig. 7b closely follow the previously discussed ones, so that the corresponding conclusions are supported.

3) Converter Setup: While the supercapacitor still serves the node and is connected to one of the ADC ports, the

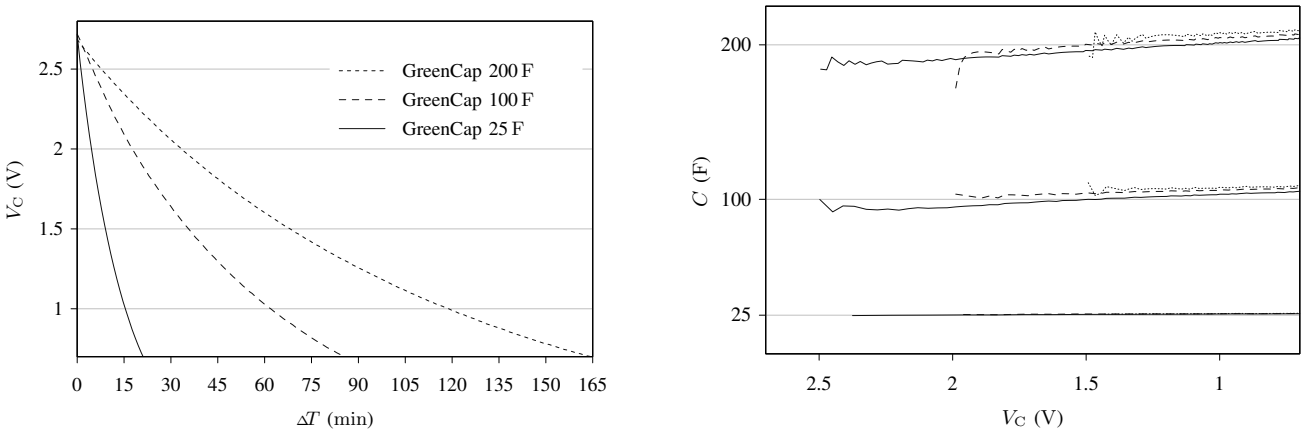

(a) Process of voltage

(b) Capacity estimation for increasing ΔV_C

Fig. 5. Plain resistance discharging without sensor node ($R = 36.1\,\Omega$)

resistance is disconnected by opening the board's switch S. The node runs in high power mode, i.e., the radio is switched on permanently. With a constant voltage of $V_N = 3.3\,V$ and an average current of $I_N = 15.8\,mA$, the node's power consumption evaluates to $P_N = 52.1\,mW$. In order to estimate the capacity with (6) we obtain the expected efficiency η from the TPS61221 data sheet. For the three (input) reference voltages and the stated output current, the determined values of η are 85%, 88% and 91%. The results of the measurements are shown in Fig. 8.

The supercapacitor voltage (Fig. 8a) decreases in a square-root shape. As compared to the resistance method, discharging is slower for large voltages, where the power of the converter approach is smaller; whereas it is faster for smaller voltages due to higher power consumption. Thus, overall discharging time is considerably lower for this approach. However, capacity determination can achieved within competitive time as compared to the resistance method.

Figure 8b implies that capacity estimation for the converter approach fails at first glance; yet, this is not true. First of all, estimations become generally stable within less than the desired $0.1\,V$. This hints at the subordinate relevance of both leakage current and the falling efficiency with decreasing input voltage. Since they are influencing the results at different voltages, their effects could be evenly distributed over the full voltage range. The influence of the latter is also alleviated by the long-term averaging for $V_{C0} = 2.5\,V$ and $V_{C0} = 2.0\,V$ and the small decrease in efficiency. Only at very low input voltages and for $V_{C0} = 1.5\,V$, the efficiency degeneration can be observed clearly.

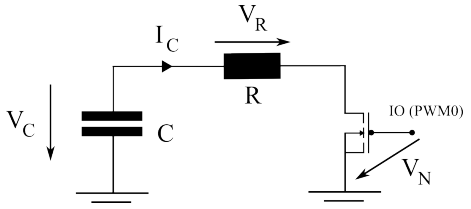

Fig. 6. Discharging circuit with MOSFET-controlled resistance

These observations plus the almost constant error of the capacities suggest that the efficiencies, i.e., input powers, are wrong, since they have a linear influence on capacity estimation, cf. (6). We have therefore investigated this matter at more detail. Firstly, we recorded the effective efficiency for the given application (switched on radio) with a voltage source and a multimeter to obtain the input power. We took these values to calculate the efficiencies $\eta(V_C)$, which are displayed in Fig. 9a. Clearly, the empirical data depart from the data sheet values, e.g., the actual efficiency for $V_C = 2.0\,V$ is as low as 73.6%. It thus shows that the overall circuit-efficiency is considerably lower than the sole converter efficiency.

Motivated by this, we recalculated the capacity estimations, that are displayed in Fig. 9b. These new results indicate that the method of converter discharging is applicable in principle, i.e., if the circuit's efficiency is known precisely. Unfortunately, this cannot be guaranteed, so that the converter method is infeasible in practice. Furthermore, estimations for $V_{C0} = 2.5\,V$ are still falling short. At the beginning of the measurement this is presumably due to the leakage current of the supercapacitor, which is in the order of a few mA and thus has a noticeable influence. The remainder of the curve is not rising, since the decrease of efficiency is not considered.

Although the previously reported findings appear to be unfruitful, there is a different yet profitable application for (6): For lifetime prediction of supercapacitors, not only the capacitance but also the efficiency of the complete supply is of relevance. Once the actual capacitance is known, there still is a lack of this latter knowledge. Here, the efficiency encompasses the overall efficiency of the supply, i.e., all losses have to be taken into account, including the conversion losses plus capacitor's self-discharge (leakage power). If the capacitance is known—this can be achieved with the resistance-discharging method—the supply's efficiency can be determined via fixed-power discharging. Since the efficiency has an almost linear

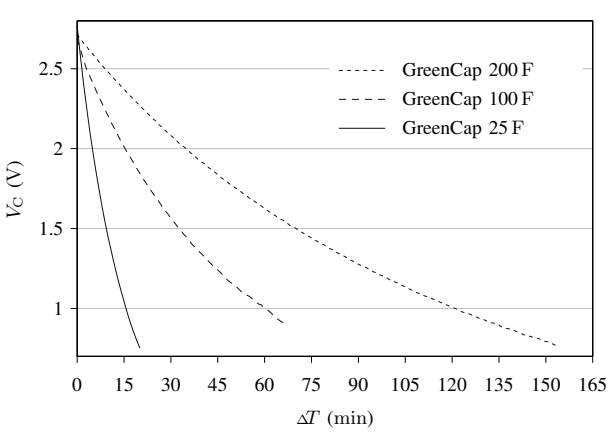

(a) Process of voltage

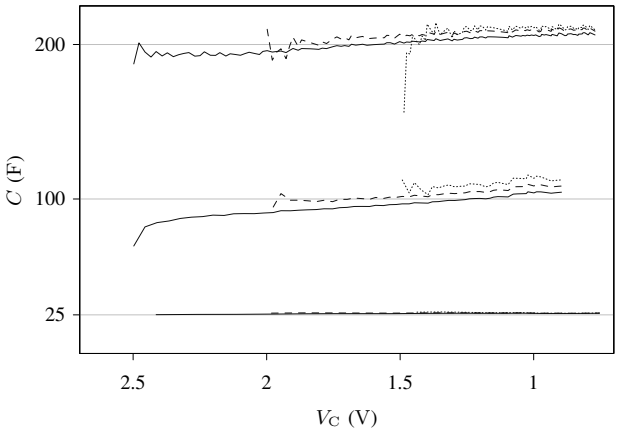

(b) Capacity estimation for increasing ΔV_C

Fig. 7. MOSFET-controlled resistance discharging ($R = 35.6\,\Omega$)

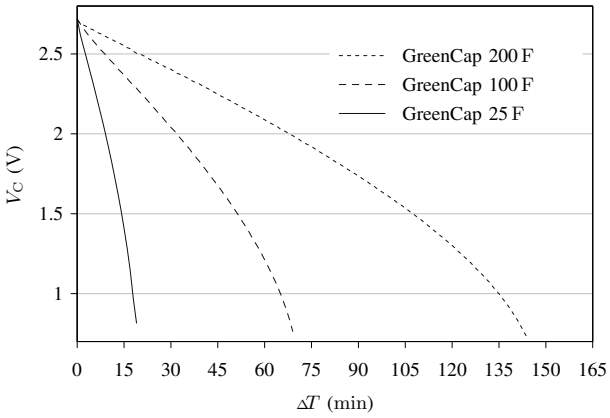

(a) Process of voltage

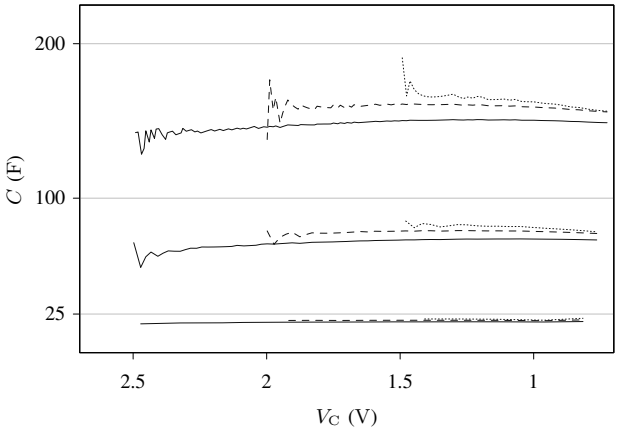

(b) Capacity estimation for increasing ΔV_C

Fig. 8. Converter discharging with converter efficiency values taken from the data sheet

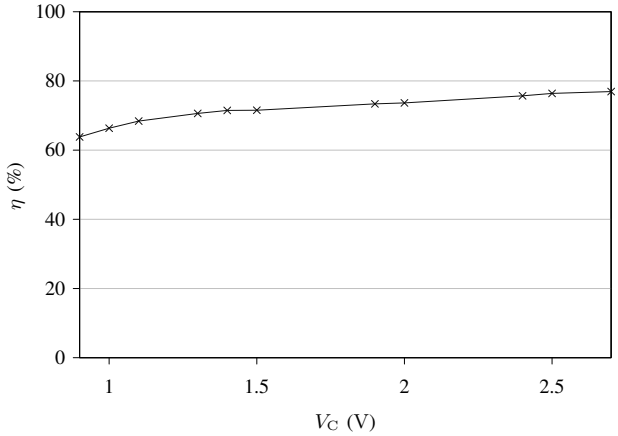

(a) Measured DC-DC efficiency

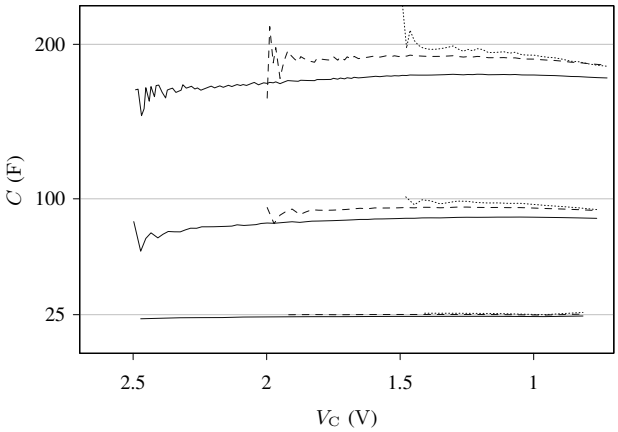

(b) Capacity estimation for increasing ΔV_C

Fig. 9. Converter discharging with measured circuit efficiency values

shape for $V_C \geq 1.2\,V$ (cf. Fig. 9a) and leakage power has a high impact for large values of V_C only, it could be possible to easily derive a lower bound on overall efficiency in order to improve lifetime prediction for the harvesting platform under consideration.

B. A Roadmap for a Self-Calibration Algorithm

The discoveries of the first part of this section furnish a concept for online capacitance determination. Resistance discharging is a fast and reliable tool on this matter. A voltage drop ΔV_C of $0.1\,V$ is sufficient to determine the capacity at reference voltages in the area of $2\,V$, which leaves the hardware with enough energy so as not to provoke energy shortage. At a node's boot time, a setup routine is executed, that triggers capacitance determination once the needed voltage is available. At this point, the node must not perform any other tasks, and it checks the voltage periodically, until the needed voltage drop is observed. Then, the capacity can be estimated using (3). Afterwards, the efficiency of the power supply can be determined by fixed-power discharging and (6), possibly for different powers, e.g., considering the sleeping and the idle (listening) radio mode. Once this procedure is finished, self-calibration is completed and reliable lifetime prediction becomes possible. We encourage the application of such a self-calibration phase although the measurements have shown that there is no great deviation from the nominal capacity values. The reason for this is many-fold, where the most important points are the following. Firstly, environment conditions, such as temperature, may influence the actual capacity (we have conducted our measurements at room temperature only). Secondly, the efficiency of the supply circuit is subject to manufacturing fluctuation, so that it has to be determined for each device. Thirdly, this approach frees from manual configuration, so that nodes can be equipped with any capacity or supply circuit without any manual gauging.

Due to the changing environmental conditions, the aging of the supercapacitor and of the whole supply circuit with all its components, recalibration will be required sooner or later. For this purpose we envision two simple mechanisms. Firstly, periodical service intervals could be a feasible and easy way to go. Service intervals could be prolonged and shortened, depending on the actual change of current and past estimations of capacity and efficiency. Secondly, the quality of the estimates can be assessed as follows. Lifetime predictions for some given minimum voltage—that is way larger than the minimum cut-off voltage of the DC-DC-converter—could be compared with the actual time passed until reaching the desired voltage level. In case of a large error, a recalibration is triggered. Of course, this approach is only possible, if there is no incoming energy. In case of the application of a solar cell, the night reveals itself as a candidate time for performing the described check.

The just sketched approach is currently implemented and evaluated by the authors of this paper.

VII. Conclusion

With this contribution we have continued the work started in [1]: the realization of self-sustaining wireless sensor nodes that use the available energy resources as effectively as possible without exposing themselves to the hazard of accidental energy depletion. For this purpose, we have revisited the underlying hardware platform and analyzed the theoretical model of lifetime prediction. The capacity of supercapacitors, serving as energy buffers, varies greatly from its initial value. Therefore, it must be determined and updated dynamically, since its value influences the precision of lifetime prediction directly without interrupting normal operation and with little energy cost. This also has the benefit that nodes can be equipped with virtually any supercapacitor devoid of the need of manual configuration.

To achieve this goal, we have discussed two different models for capacity estimation. The first one uses a separate resistance for controlled, partly discharging of the capacitor. The second one does not need any extra hardware, but discharges the capacity via the DC-DC-converter needed to supply the node with a constant voltage. In this context, we have analyzed the time needed for self-calibration depending on the actual capacity, the resistance, the power consumption of the sensor node, and the voltage drop. Additionally, the accuracy of the calculated capacities has been estimated with respect to the measurement precision achievable with the ADC of the platform. It shows that the combination of a $40\,\Omega$ resistance and a voltage drop of $0.1\,V$ meets the requirements of fast capacity determination and low voltage drop—i.e., energy loss due to measuring—while approximately reflecting the sensor node's current profile. Our assessment also shows that resistance discharging is usually faster than converter discharging while not relying on external influences, such as the converter's efficiency.

In addition to the theoretical analysis, measurements have been performed for an existing hardware platform. They reveal that resistance discharging is a reliable method for capacity estimation. The results also show that using a reference voltage of ca. $2\,V$ is a good choice to achieve fast and sufficiently precise capacity values. Contrarily, the converter method relies massively on the whole power-supply circuit's efficiency; hence, it cannot be used for capacity determination. The good news, none the less, is that both methods can be combined effectively. While resistance discharging can be used to estimate the capacity, converter discharging can be employed to determine the circuit's efficiency for different voltages of the supercapacitor and different current profiles of the sensor node, the two main driver's of the circuit's efficiency. These findings are of high value, since they pave the way for reliable lifetime prediction and therefore energy-budgeting for wireless sensor nodes and other mobile devices.

Acknowledgment

This research has been partially funded by the German Research Foundation (Deutsche Forschungsgemeinschaft, DFG) under contract number TU 221/4-1. The authors would also

like to thank Leo Krüger for his assistance in taking measurements and developing the test software.

REFERENCES

[1] C. Renner, J. Jessen, and V. Turau, "Lifetime Prediction for Supercapacitor-powered Wireless Sensor Nodes," in *Proc. of the 8th GI/ITG KuVS Fachgespräch "Drahtlose Sensornetze" (FGSN '09)*, Hamburg, Germany, Aug. 2009.

[2] Panasonic, *Gold Capacitors Technical Guide*. [Online]. Available: http://www.panasonic.com/industrial/components/pdf/goldcap_techguide_052505.pdf

[3] Samwha Capacitor Group, *Green Caps – Datasheet*. [Online]. Available: http://www.samwha.com/electric/templatedirs/guest/list_pdf1/DP.pdf

[4] V. Kyriatzis, N. S. Samaras, P. Stavroulakis, H. Takruri-Rizk, and S. Tzortzios, "Enviromote: A New Solar-Harvesting Platform Prototype for Wireless Sensor Networks / Work-in-Progress Report," in *Proc. of the Annual IEEE International Symposium on Personal, Indoor and Mobile Radio Communications (PIMRC '07)*, Athens, Greece, 2007.

[5] Crossbow Technology, *IRIS Wireless Measurement System – Datasheet, Rev. A*. [Online]. Available: http://www.xbow.com/Products/Product_pdf_files/Wireless_pdf/IRIS_Datasheet.pdf

[6] C. Lange, "Energiegewinnung für drahtlose Sensorknoten (Diploma Thesis)," Master's thesis, Hamburg University of Technology, Oct. 2008.

[7] X. Jiang, J. Polastre, and D. Culler, "Perpetual Environmentally Powered Sensor Networks," in *Proc. of the 4th Intl. Symposium on Information Processing in Sensor Networks (IPSN '05)*, Los Angeles, CA, USA, Apr. 2005.

[8] P. Dutta, J. Hui, J. Jeong, S. Kim, C. Sharp, J. Taneja, G. Tolle, K. Whitehouse, and D. Culler, "Trio: Enabling Sustainable and Scalable Outdoor Wireless Sensor Network Deployments," in *Proc. of the 5th Intl. Conf. on Information Processing in Sensor Networks (IPSN '06)*, Nashville, TN, USA, Apr. 2006.

[9] F. Simjee and P. H. Chou, "Everlast: Long-Life, Supercapacitor-Operated Wireless Sensor Node," in *Proc. of the Intl. Symposium on Low Power Electronics and Design (ISLPED '06)*, Tegernsee, Germany, 2006.

[10] V. Raghunathan, A. Kansal, J. Hsu, J. Friedman, and M. Srivastava, "Design Considerations for Solar Energy Harvesting Wireless Embedded Systems," in *Proc. of the 4th Intl. Symposium on Information Processing in Sensor Networks (IPSN '05)*, Apr. 2005.

[11] J. Jeong, X. F. Jiang, and D. E. Culler, "Design and Analysis of Micro-Solar Power Systems for Wireless Sensor Networks," in *Proc. of the 5th Intl. Conf. on Networked Sensing Systems (INSS '08)*, Kanazawa, Japan, Jun. 2008.

[12] P. Barrade and A. Rufer, "Current Capability and Power Density of Supercapacitors: Considerations on Energy Efficiency," in *Proc. of the 10th European Conference on Power Electronics and Applications (EPE '03)*, Sep. 2003.

[13] Texas Instruments, *TPS 61200 – Datasheet*, Feb. 2008. [Online]. Available: http://focus.ti.com/lit/ds/symlink/tps61200.pdf

[14] ——, *TPS 61221 – Datasheet*, Jan. 2009. [Online]. Available: http://focus.ti.com/lit/ds/symlink/tps61221.pdf

[15] V. Siliconix, *Si9410BDY N-Channel 30-V (D-S) MOSFET – Datasheet*. [Online]. Available: http://www.vishay.com/docs/72269/72269.pdf